**INTERNATIONAL JOURNAL OF OPTIMIZATION IN CIVIL ENGINEERING**
***Int. J. Optim. Civil Eng., 2014; 4(1):93-119***

# OPTIMAL SENSOR PLACEMENT FOR MODAL IDENTIFICATION OF A STRAP-BRACED COLD FORMED STEEL FRAME BASED ON IMPROVED GENETIC ALGORITHM

F. Zahedi Tajrishi[*, †,a] and A. R. Mirza Goltabar Roshan[a]
[a]*School of Civil Engineering, Babol University of Technology, Mazandaran, Iran*

## ABSTRACT

This paper is concerned with the determination of optimal sensor locations for structural modal identification in a strap-braced cold formed steel frame based on an improved genetic algorithm (IGA). Six different optimal sensor placement performance indices have been taken as the fitness functions; two based on modal assurance criterion (MAC), two based on maximization of the determinant of a Fisher information matrix (FIM), one aim on the maximization of the modal energy and the last is a combination of two aforementioned indices. The decimal two-dimension array coding method instead of binary coding method is applied to code the solution. Forced mutation operator is applied whenever the identical genes produce via the crossover procedure. An improvement is also introduced to mutation operator of the IGA. A verified computational simulation of a strap-braced cold formed steel frame model has been implemented to demonstrate the effectiveness and application of the proposed method. The obtained optimal sensor placements using IGA are compared with those gained by the conventional methods based on several criteria such as norms of FIM and minimum in off-diagonal terms of MAC. The results showed that the proposed IGA can provide sensor locations as well as the conventional methods. More important, based on the criteria, four of the six fitness functions, can identify the vibration characteristics of the frame model accurately. It is shown through the example that in comparison with the MAC-based performance indices, the use of the FIM-based fitness functions results in more acceptable and reasonable configurations.

Received: 25 October 2013; Accepted: 15 March 2014

KEY WORDS: Optimal sensor placement, improved genetic algorithm, cold formed steel, strap brace, modal analysis, modal assurance criterion

[*]Corresponding author: F. Zahedi Tajrishi, Phd Student, School of Civil Engineering, Babol University of Technology, Mazandaran, Iran, Tel (+98-912) 2155689.
[†]E-mail address: : f.zaheditajrishi@stu.nit.ac.ir (F. Zahedi Tajrishi)

## 1. INTRODUCTION

Parameter identification is a main part of health monitoring, model updating and control of structures. Modal parameters, consisting of mode shapes and modal frequencies, are kind of structural parameters which can used to describe the dynamic behavior of a structural system. In order to investigate the modal parameters of a structure accurately, selection of target modes and sensor placements are the main important factors. In particular, the robustness of modal parameter identification strongly depends on the robustness of the measured vibration data, which are dependent on the locations of sensors in the structure [1]. Therefore determining the optimal sensor placement (OSP) has a key role in an accurate modal parameter identification process. OSP process provides the condition under which modes can be clearly identified with the most valuable information [2].

In the past two decades, various techniques and criteria have been developed for OSP of the structures. In most cases, an optimal configuration is one which provides the best observability and distinguishability for the identified target modes [3]. For example, approaches based on maximization of the determinant of the Fisher information matrix (FIM) [4, 5] and minimization of the off-diagonal terms of the modal assurance criterion (MAC) matrix [6]. One of the most common OSP methods called the effective independence (EFI) method used for the structural modal identification was developed by Kammer in 1991 [4]. The method starts with a relative large candidate set for sensor places, ranks all the candidate places based on their contributions to the determinant of a FIM, and then removes the lowest ranked candidate. The new reduced candidate sensor set is then re-ranked and the place with the lowest rank is again eliminated. This process continues until the initial candidate set is reduced to the certain number of sensors. Cherng accelerated the optimization process by a backward deletion algorithm [2]. Kammer also presented a method iteratively expands an initial set of sensors instead of iteratively reducing a large candidate set for triaxial sensor set selection [7]. Li and Fritzen [8] addressed the connection between EFI and modal kinetic energy (MKE) methods for sensor placement. Li et al. [9] proposed an extension of the minMAC algorithm to aid sensor placement for modal tests. Tang and Li [10] presented a method based on the uniform design theory to optimize sensor locations for structural vibration measurements. Cherng [2] used signal subspace correlation to optimize the sensor placement for modal identification. Papadimitriou [1] used the information entropy as the performance measure of a sensor configuration. He also developed appropriate information entropy indices as the optimality criteria for pareto optimal sensor configurations for multiple model classes [11].

In recent years, computational intelligence methods have been applied for OSP of the structures. One example is genetic algorithm (GA) based on the theory of biological evolution [12]. GA has been an effective alternative to the previous heuristic algorithms which are not guaranteed to give the optimal result for the problem of sensor placement. Yao et al. [12] took GA as an alternative to the EFI method with the determinant of the FIM as the fitness function. Papadimitriou and Beck [13] used a GA to minimize the entropy measure as the optimality criterion over the set of possible sensor configurations. Vosoughifar et al. [14, 15] used GA for the optimal sensor placement of two different systems, i.e. light steel frame system and steel structure with unbonded braced frame system

to identify the dynamic parameters of the systems. Although GA has been proved to be a powerful tool for OSP, it still has some faults need to be improved [12, 16, 17 and 18]. When GA is applied to OSP, the general crossover and mutation operators may produce generations which don't satisfy the constraints [3]. Different genetic operators, such as force mutation [12], filter operator [16] and Partially Matched Crossover [17], have been presented to improve these defects. Some researches have been made to improve GA by another artificial intelligence method. For example, Javadi et al. [18] presented a hybrid intelligent GA which was based on a combination of neural network and GA. Hwang and He [19] used simulated annealing and adaptive mechanism to improve the convergence speed and to insure the solution quality. In order to improve the convergence speed and avoid premature convergence, virus evolutionary theory [20-24] was introduced into partheno-genetic algorithm. There are also some attempts to use GA for the OSP problems with some improvements. For example, Liu et al. [25] introduced an improved genetic algorithm to find the optimal placement of sensors and proposed to code the solution by the decimal two-dimension array coding method instead of binary coding method. The results of a computational simulation of a 12-bay plain truss model showed that proposed GA could enlarge the genes storage and improve the convergence of the algorithm. Kang et al. [3] introduced virus coevolution partheno-genetic algorithms which combined a partheno-genetic algorithm with virus evolutionary theory to place sensors optimally on a large space structure for the purpose of modal identification. YI et al. [26] proposed generalized genetic algorithm to find the optimal placement of sensors for the tallest building in the north of the China. The dual-structure coding method instead of binary coding method was proposed to code the solution, which could improve the convergence of the algorithm and get the better placement scheme. Yi et al. [27] presented a hybrid method based on multiple optimizations. The initial sensor placement was firstly obtained by the QR factorization. Then, using the minimization of the off-diagonal elements in the MAC, the quantity of the sensors was determined by the forward and backward sequential sensor placement algorithm together. Finally, the locations of the sensor were determined by the dual-structure coding-based generalized genetic algorithm.

The research presented in this paper applied an improved genetic algorithm (IGA) to find the best solution for the problem of placing certain numbers of sensors for modal identification of a strap-braced cold formed steel (CFS) frame. The layout of the paper is as follows: Section 2; gives the basic theory of the IGA including the selection of the fitness functions, the presented coding system, genetic operators and convergence criteria. Section 3 describes the computational simulation using a strap-braced cold formed steel frame model; The result of presented optimization strategy is demonstrated and compared with the results obtained by three conventional methods effective independence (EFI), effective independence-driving point residue (EFI-DPR) and minMAC, in Section 3. Different evaluation criteria are applied to assess the results obtained by aforementioned methods in Section 4. Finally, in Section 5, based on the results, the appropriate methods for OSP of the CFS frame are proposed and the optimal configurations of sensors are presented.

## 2. IMPROVED GENETIC ALGORITHM

Genetic algorithm is an optimization technique based on the principles of natural selection and genetics. A GA allows a population composed of many individuals to evolve under specified selection rules to a state that maximizes the fitness function [28]. The method was developed by John Holland in 1975 [29] and finally popularized by David Goldberg in 1989 [30]. Since then, many versions of evolutionary programming have been tried with varying degrees of success. The GA process is initiated by defining the optimization variables and the fitness function. It continues by creation of an initial population from input variables, either heuristically or randomly. Then the initial population is encouraged to evolve over generations to produce new designs, which are better or fitter. The quality or fitness of the designs is evaluated according to the fitness function. Finally, it ends by testing for convergence.

However GA has been proved to be a powerful tool for OSP, there are still some shortcomings which decrease the efficiency of the method. For example, when GA is used for OSP problem, the general crossover and mutation operators may generate chromosomes that do not satisfy the constraints. One location may be occupied by two or more sensors causing the number of sensors to become less than the desired certain number. Therefore, some improvements are implemented to GA in the frame of improved genetic algorithm (IGA) to overcome these difficulties.

### *2.1 Defining variables*

The IGA process is initiated by defining the input variables to be optimized. To apply IGA to the OSP for modal identification of the CFS frame, input variables are defined as the possible degrees of freedom (DOFs) for sensor locations. Each DOF with this ability is represented as an integer (the "gene"). If there are ***m*** sensors to be placed in the total ***s*** degrees of freedom, therefore ***m*** genes are concentrated into an integer string (the " chromosome") with the coding length of ***m***. Each value of the string is the number of DOF on which the sensor is located. Each chromosome represents a possible set of DOFs for sensor locations. For example in a system which is needed to have five sensors in optimal locations, the chromosome of "3 5 6 10 14" means that five sensors located on 3rd, 5th, 6th, 10th, and 14th DOFs (the " genes") of the structure. Several chromosomes in a matrix make a "population". At the first generation of IGA, initial population is produced randomly or heuristically but in the next generations, it is reproduced by IGA operators. If the size of the initial population of individuals is ***k***, then the population is formed as Table 1:

Table 1: The decimal two- dimension array coding system for *m=8*.

| | No of gene: | 1 | 2 | 3 | 4 | 5 | 6 | 7 | 8 |
|---|---|---|---|---|---|---|---|---|---|
| population | chromosome 1: | 11 | 12 | 53 | 54 | 116 | 117 | 158 | 159 |
| | chromosome 2: | 13 | 15 | 61 | 72 | 100 | 121 | 154 | 160 |
| | .... | ... | ... | ... | ... | ... | ... | ... | ... |
| | chromosome k: | 10 | 13 | 54 | 63 | 109 | 131 | 159 | 166 |

in which the number of sensors ***m*** is 8 and the total DOFs ***s*** is 168 in this paper. (Referred to the illustrative example presented subsequently in Section 3).

This coding system named the decimal two-dimension array coding system is the first improvement applied to the simple GA in this paper. To demonstrate the advantage of the decimal coding method in order to reduce the requirement for the storage space, two binary coding methods are introduced as Tables 2 and 3. Table 2 shows one kind of binary coding method in which the coding length of a string is the total DOFs ***s***. If the value of the *i*th bit position of the string is ***1***, it denotes that a sensor is located on the *i*th DOF. In contrast, if the value of the *i*th bit position is ***0***, it denotes that there is no sensor on the *i*th DOF [31]. Table 3 shows another kind of binary coding method in which one sensor location is represented by a binary string, and then all the strings are connected in series as a total string [25]. Liu et al. showed that the dissipative storage space of the decimal two-dimension array coding method is minimal as well as its convergence is the best among the aforementioned existing GA coding systems [25].

### *2.2 Defining fitness function*

The IGA aims to find a set of DOFs, as the "best" chromosome, for sensor locations to maximize the fitness function. The fitness function generates an output from a set of input variables. In this case the fitness functions are defined in six different fitness models:

1 and 2-modal assurance criterion (MAC): The MAC can be defined as Eq. (1), which measures the correlation between mode shapes.

$$MAC_{ij} = \frac{\left(\phi_i^T \phi_j\right)^2}{\left(\phi_i^T \phi_i\right)\left(\phi_j^T \phi_j\right)} \tag{1}$$

where $\phi_i$ and $\phi_j$ represent the *i*th mode shape vector and the *j*th mode shape vector, respectively, and the superscript *T* represents the transpose of the vector.

For an optimal sensor configuration, the MAC matrix will be diagonal. Therefore, the size of the off-diagonal terms of MAC is a criterion for performance of OSP and can be considered as an indication of fitness function. In this study the MAC matrix is used to construct two fitness functions. The first is the average value of all the off-diagonal elements in MAC matrix and the second is the biggest value in all the off-diagonal elements in MAC matrix. The first fitness function made of MAC named $f_1$ is given as Eq. (2) and the second fitness function $f_2$ is taken as Eq. (3).

$$f_1 = 1 - average(abs(MAC_{ij})), \qquad i \neq j \tag{2}$$

$$f_2 = 1 - \max(abs(MAC_{ij})), \qquad i \neq j \tag{3}$$

where average (.) represents the average value, abs (.) represents the absolute value and max (.) represents the maximal value.

Table 2: The first binary coding system for the chromosomes of Table 1.

| No of gene: | 1 | 2 | ... | 10 | 11 | 12 | 13 | 14 | ... | 53 | 54 | 55 | ... | 116 | 117 | ... | 158 | 159 | 160 | ... | 168 |
|---|---|---|---|---|---|---|---|---|---|---|---|---|---|---|---|---|---|---|---|---|---|
| chromosome 1: | 0 | 0 | 0 | 0 | 1 | 1 | 0 | 0 | 0 | 1 | 1 | 0 | ... | 1 | 1 | 0 | 1 | 1 | 0 | 0 | 0 |
| chromosome 2: | 0 | 0 | 0 | 0 | 0 | 0 | 1 | 0 | ... | 0 | 0 | 0 | ... | 0 | 0 | ... | 0 | 0 | 1 | ... | 0 |
| ... | . | . | ... | ... | ... | ... | ... | ... | ... | ... | ... | ... | ... | ... | ... | ... | ... | ... | ... | ... | ... |
| chromosome k: | 0 | 0 | 0 | 1 | 0 | 0 | 1 | 0 | 0 | 0 | 1 | 0 | ... | 0 | 0 | ... | 0 | 1 | 0 | ... | 0 |

Table 3: The second binary coding system for the chromosomes of Table 1.

| Population | No of gene: | 1 | 2 | ... | 7 | 8 |
|---|---|---|---|---|---|---|
| | chromosome 1: | 11010000 | 00110000 | ... | 01111001 | 11111001 |
| | chromosome 2: | 10110000 | 11110000 | ... | 01011001 | 00000101 |
| | ... | ... | ... | ... | ... | ... |
| | chromosome k: | 01010000 | 10110000 | ... | 11111001 | 01100101 |

3- The effective independence (EFI) index: According to structural dynamics [32], the mathematical model for OSP of an elastic structure can be defined in the uncoupled modal form:

$$\begin{aligned} &\ddot{q} + M^{-1}C\dot{q} + M^{-1}Kq = M^{-1}\Phi^T F \\ &y = \Phi q + \varepsilon \end{aligned} \tag{4}$$

where $q \in R^N$ represents the modal coordinate vector; **M**, **K**, $C \in R^{M\times N}$ are modal mass, stiffness and damp matrix of the structure, respectively; $\Phi \in R^{M\times N}$ is the mode shape matrix, whose column represents mode shape vector; $F \in R^M$ is the force vector; The superscripts -1 and T denote the inversion and transpose of a matrix, respectively; $y \in R^M$ is the normal coordinate vector; $\varepsilon \in R^M$ is the sensor noise vector, which is often assumed to be a stationary Gaussian white noise with zero mean and positive definite covariance intensity matrix $R \in R^{M\times M}$ such that:

$$E\left[\varepsilon(t)\varepsilon(\tau)^T\right] = R\delta(t-\tau) = diag((\sigma^2)_M) \tag{5}$$

where $E$ is the expectation operator; $\sigma$ represents the standard deviation of Gaussian white noise and $diag((\sigma^2)_M)$ shows the diagonal matrix whose the all diagonal terms are $\sigma^2$.

Eq. (4) indicates that the response in any point of an elastic structure can be obtained as a linear combination of mode shape values. In this case, the *i*th coefficient of *y* is a linear combination of *i*th mode shape vectors, where $q_i$ is a function either of time or frequency and acts as a multiplier coefficient. By an efficient unbiased estimator to evaluate the coefficient response vector, the covariance matrix of the estimate error is given by:

$$C = E\left[(q-\hat{q})(q-\hat{q})^T\right] = \left[\frac{1}{\sigma^2}\Phi_m^T\Phi_m\right] = F^{-1} \tag{6}$$

where **C** represents the covariance matrix, **F** is the Fisher information matrix (FIM), $\hat{q} = \left[\Phi_m^T\Phi_m\right]^{-1}\Phi_m^T y_m$ denotes the vector of an efficient unbiased estimator of ***q*** and ***m*** is the number of desired sensor locations. Since the best estimation of ***q*** occurs when **F** is maximized, therefore the procedure for selecting the best sensor placement is to select the candidate sensors such that the determinant of the FIM will be maximized. In order to achieve this, the third fitness function can be defined as Eq. (7).

$$f_3 = \det(F) = \det(\phi^T\phi) \tag{7}$$

4- The EFI- driving point residue (EFI-DPR) index: A limitation of the EFI index -based method is that sensor locations with low energy can be selected, which decreases the signal

to noise ratio causing the difficulty in mode shape identification. The EFI-DPR index eliminates this problem by weighting the EFI indices with the corresponding DPR [33]:

$$DPR = \Phi \otimes \Phi^T \Omega^{-1} \tag{8}$$

where $\otimes$ shows a term-by- term matrix multiplication. $\Omega$ is a column vector consisting of circular frequencies corresponding to $\Phi$, and $\Omega^{-1}$ denotes the inverse of each term in $\Omega$. DPR evaluates the average contribution of a candidate location sensor to the mode shapes. By consideration of DPR, the third fitness function changes to the fourth fitness function as Eq. (9).

$$f_4 = \det(\phi^T \phi \Omega^{-1}) \tag{9}$$

5- The modal energy based index: When data are noise contaminated, the signal to noise ratio (SNR) can effect on accuracy of measured data. In this case, increasing the energy of target mode shapes raises SNR and thus improves the modal identification process [2]. Based on SNR, Cheng proposed backward deletion algorithm (BDA) which is a modal energy based method [2]. It is proposed to normalize each mode shape before ranking to eliminate the energy gap among them. Therefore the modes are treated equally before ranking. This can be done by Eq.(10).

$$\rho_{ir} = \frac{\phi_{ir}^2}{\sum_{i=1}^{m} \phi_{ir}^2} = \frac{\phi_{ir}^2}{\left\| \phi_r \right\|^2} \tag{10}$$

where $\rho_{ir}$ is the normalized contribution of the *i*th sensor placement to the *r*th mode shape, $\phi_r$ is the *r*th mode shape and $\phi_{ir}$ is the *i*th element of $\phi_r$.

The contribution matrix $\Gamma$ can be defined as follows:

$$\Gamma = \begin{bmatrix} \rho_{11} & \rho_{12} & \cdots & \rho_{1n} \\ \rho_{21} & \rho_{22} & \cdots & \rho_{2n} \\ \cdots & \cdots & \cdots & \cdots \\ \rho_{m1} & \rho_{m2} & \cdots & \rho_{mn} \end{bmatrix} \tag{11}$$

The ranking index $\Psi$ can be showed as follows:

$$\Psi = \prod_{r=1}^{n} \sum_{i=1}^{m} \rho_{ir} \tag{12}$$

Eq. (12) indicates that the modal contribution can be evaluated mode by mode.

Therefore, the fifth fitness function can be selected as:

$$f_5 = \alpha \prod_{r=1}^{n} \sum_{i=1}^{m} \rho_{ir} \tag{13}$$

where α is a parameter to tune the fitness values into an appropriate range.

6. A combined index: A drawback of the EFI method is that sensor places with low energy content can be selected with a consequent possible loss of valuable information. In order to eliminate this problem, the combined method of EFI and BDA proposed by Kang et al. [3], is taken as the sixth fitness function:

$$f_6 = f_3 \times f_5 = \beta \det(\phi^T \phi) \prod_{r=1}^{n} \sum_{i=1}^{m} \rho_{ir} \tag{14}$$

where β is a parameter to tune the fitness values into an appropriate range. This fitness function means that the selected sensor locations not only maximize the spatial independence but also maximize the modal energy.

### *2.3 IGA operators*

The IGA has three main operators: parent selection, crossover & forced mutation, and mutation.

#### *2.3.1 Parent selection*

Natural selection occurs each generation or iteration of the algorithm. If ***Npop*** is the number of population and ***Nkeep*** is the number of chromosomes which are survived from one generation to next. Of the ***Npop*** chromosomes in a generation, only the top ***Nkeep*** (with the highest fitness values) survive for mating, and the bottom ***Npop - Nkeep*** are discarded to make room for the new offspring. Chromosomes of ***Nkeep*** are kept in mating pool and parents are selected among them. There are numbers of parent selection schemes commonly used in GA. These include proportionate reproduction, ranking selection, tournament selection, steady state selection, and greedy over-selection. In this study, tournament selection is used which is closely mimics mating competition in nature. Tournament selection approach is to randomly pick a small subset of chromosomes (two or three) from the ***Nkeep*** of mating pool, and the chromosome with the highest fitness in this subset becomes a parent. The tournament repeats for every parent needed.

#### *2.3.2 Crossover and forced mutation*

Crossover is the operator that produces new offspring by exchanging some genes of a couple of parents. There are several methods to do this for example: one-point crossover, two point crossover, scattered crossover and so on. Figure 1 shows the two-point crossover operation which is used in this study. As shown in Figure 1, first, two random points are chosen among genes of the parents; the point ***1*** is chosen between the genes two and three, and the

point ***2*** is chosen between the genes six and seven. The first parent's genes are depicted by bold numbers while the second parent's genes are shown by italic numbers. When crossover applied, the first parent's genes before point ***1*** and after point ***2*** are transferred to offspring one as depicted by the Figure. The other genes of the first parent are located on offspring ***2***. The process is reversed for the genes of the second parent. More detailed of this method are discussed in reference [30]. In some cases, however the parent strings satisfy the constraint, the new offspring may still violate the constraint. In this case, the same DOF may be occupied by two or more sensors synchronously which is impractical and must be avoided in the crossover process. Therefore, forced mutation [28] is applied to improve the crossover operator. The detailed operation process is presented and shown in Table 4. The first two lines in Table 4 are the two selected parents which are mated by two-point crossover method. The two new offspring will be generated as shown in the second two lines in Table 4. Unfortunately, the 6th gene of one new offspring (offspring 1) is the same with the 7th gene of it (the underlined numbers). That means one DOF (number 122) has been placed with two sensors synchronously. So the forced mutation operator is introduced to change one value of the same two numbers to the other value, which is not included in the offspring 1. In this example, the second value 122 is changed to 135 (the bold underlined number in the fifth line in Table 4), which is different from other genes in the offspring 1.

| | | | | Point 1 | | | | Point 2 | |
|---|---|---|---|---|---|---|---|---|---|
| | | 1 | 2 | 3 | 4 | 5 | 6 | 7 | 8 |
| chromosome pair before crossover | Parent 1 | **10** | **23** | **45** | **62** | **89** | **93** | **122** | **149** |
| | Parent 2 | *11* | *31* | *45* | *55* | *74* | *122* | *134* | *167* |
| chromosome pair after crossover | Offspring 1 | **10** | **23** | *45* | *55* | *74* | *122* | **122** | **149** |
| | Offspring 2 | *11* | *31* | **45** | **62** | **89** | **93** | *134* | *167* |

Figure 1. Two-point crossover operation for *m=8*.

Table 4: Operation of forced mutation in IGA for m=8.

| | | 1 | 2 | 3 | 4 | 5 | 6 | 7 | 8 |
|---|---|---|---|---|---|---|---|---|---|
| chromosome pair before crossover | Parent 1: | **10** | **23** | **45** | **62** | **89** | **93** | **122** | **149** |
| | Parent 2: | *11* | *31* | *45* | *55* | *74* | *122* | *134* | *167* |
| chromosome pair after crossover | Offspring 1: | **10** | **23** | *45* | *55* | *74* | *122* | **122** | **149** |
| | Offspring 2: | *11* | *31* | **45** | **62** | **89** | **93** | *134* | *167* |
| chromosome pair after forced mutation | Modified offspring 1: | 10 | 23 | *45* | *55* | *74* | *122* | **135** | 149 |
| | Offspring 2: | *11* | *31* | **45** | **62** | **89** | **93** | *134* | *167* |

*2.3.3 Mutation*

To apply improved mutation in this study, first the chromosomes randomly selected for mutation are encoded from decimal coding to binary coding as shown in Table 5. Then, the

mutation operation randomly selects one gene position from the ones whose value is ***1*** in a chromosome, for example DOF 45 in third row of Table 5. Then the mutation operation randomly selects another gene position from the ones whose value is ***0*** in the chromosome, for example DOF 64 in third row of Table 5. Finally, the positions of the two genes are swapped to produce an offspring. Therefore, DOF 45 as a sensor placement is converted to DOF 64 as shown in the last row of the Table. By this method the numbers of ***1*** which is an indication of the number of sensors will be unchanged. Finally, the new chromosome binary code is converted to decimal code. The improved mutation scheme is shown in Table 5. Through the operation of aforementioned crossover-force mutation and mutation, the offspring satisfy the constraints as their parents do.

Table 5: Improved mutation for m=8.

| Chromosome for mutation | 11 | | | 31 | | 45 | | 62 | | 89 | | 93 | | 134 | | 166 |
|---|---|---|---|---|---|---|---|---|---|---|---|---|---|---|---|---|
| Encoding chromosome | 1 | 2 | ... | 43 | 44 | 45 | ... | 62 | 63 | 64 | 65 | ... | 166 | 167 | 168 | |
| | 0 | 0 | | 0 | 0 | ***1*** | | 1 | 0 | ***0*** | 0 | | 1 | 0 | 0 | |
| Mutation of chromosome | 0 | 0 | | 0 | 0 | ***0*** | | 1 | 0 | ***1*** | 0 | | 1 | 0 | 0 | |
| Decoding mutated chromosome | 11 | | | 31 | | 62 | | 64 | | 89 | | 93 | | 134 | | 166 |

*2.4. IGA Convergence*

After the improved mutations take place, the fitness functions corresponding to the offspring and mutated chromosomes are evaluated. The process described is iterated in terms of generations until the convergence criteria are met. The three termination criteria are given for IGA as follows:

(1) A convergence criterion is given as $\left| fit_{\max} - fit_{avg} \right| \le \varepsilon$, where $\boldsymbol{fit_{max}}$ represents maximum fitness, $\boldsymbol{fit_{avg}}$ represents average fitness and ε is a small number.

(2) A relative large number ***N*** is selected to avoid redundant iteration. The IGA process will be stopped automatically if the fittest chromosome in the population does not change in continuous N iteration.

(3) A maximum number of generations is set to stop the process after a relative large number of iterations.

If either of the three convergence criteria is met, the genetic operation should be terminated.

The whole flowchart of the presented improved genetic algorithm for the optimal sensor placement is shown in Figure 2.

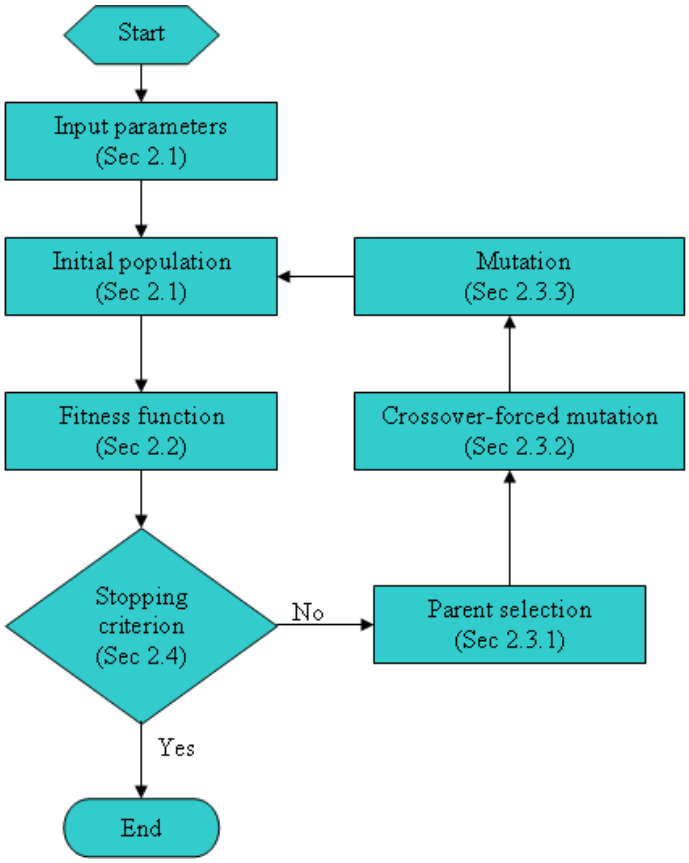


Figure 2. Flowchart of improved genetic algorithm.

## 3. NUMERICAL EXAMPLE

In this section, the proposed OSP method is applied to a two-dimensional strap-braced cold formed steel (CFS) frame as follows:

### *3.1 Description of the CFS frame model*

The CFS frame modeled in this paper is a 2.4 to 2.4 m shear wall with solid X straps on both sides connecting to the wall's corners. This frame was tested in the Structural Laboratory of the School of Civil Engineering at the University of Queensland [34]. Figure 3 shows the general configuration of the strap-braced CFS frame. All of the frame elements, such as studs, top and bottom tracks and noggins were made using an identical C-section of dimensions 90 x 36 x 0.55 mm. The detailed section geometry is depicted in Figure 4 and the section structural material properties are listed in Table 6. The dimensions, cross section and structural material properties of the straps are presented in Table 7. All studs were connected together at each flange using just one rivet. In order to increase the buckling capacity of the chords and studs, a noggin was used in the middle height of the frame. Four

brackets are added to the corners of the frame to improve wall's lateral performance characteristics; such as strength, stiffness and ductility [35].

Table 6: Mechanical properties of the C section [34].

| No. | Property | Value | No. | Property | Value |
|---|---|---|---|---|---|
| 1 | Nominal grade | 550 MPa | 5 | Yield strain | 0.45% |
| 2 | Nominal thickness | 0.55 mm | 6 | Ultimate stress $F_u$ | 617MPa |
| 3 | Elastic modulus | 169 GPa | 7 | Ultimate strain | 2.86% |
| 4 | Yield stress $F_y$ | 592 MPa | 8 | $F_u / F_y$ | 1.04 |

Table 7: Mechanical properties of the Straps [34].

| No. | Property | Value | No. | Property | Value |
|---|---|---|---|---|---|
| 1 | Nominal grade | 300 MPa | 5 | Yield stress $F_y$ | 310 MPa |
| 2 | Nominal thickness | 0.8 mm | 6 | Yield strain | 0.18% |
| 3 | Elastic modulus | 163 GPa | 7 | Ultimate stress $F_u$ | 370 MPa |

*3.2 Finite element model of the frame*

A finite element (FE) model of the CFS frame was established using commercial FE package ABAQUS [36]. The FE model shown in Figure 5 represents the frame with the geometry and structural properties corresponding to the specimen described in the last section.

All the members are modeled by shell element S4R in ABAQUS, associated with 6 DOFs in each node. Totally, 13010 nodes and 11462 elements are generated. “Tie” technique has been applied to model the rivet connections. Also in order to consider the effects of screws’ holes on the straps’ behaviour, two types of materials were defined for the straps between brackets, and between brackets and the corners, based on reference [35]. Initial imperfection which has considerable effects on nonlinear behaviour of the frame is not considered in this linear modal analysis of the frame for simplicity. Furthermore, the effect of residual stresses and perforations are small enough to be negligible in the studied frame [35] and therefore they are not applied to the model. In order to verify the model with experimental test, a pushover analysis has been carried out. Figure 6 shows the reasonable agreement between experimental and numerical pushover curves obtained from experimental results and pushover analysis, respectively. Therefore, in order to provide input data for the sensor placement, the modal analysis was carried out using frequency analysis in ABAQUS. The first six mode shapes of the CFS frame are illustrated in Figure 7. Of the first six modes, the fifth and sixth mode shapes, which are corresponding to the general frame, have been considered as target modes. The other mode shapes are attributed to the buckling modes of the straps and are not appropriate for modal identification process.

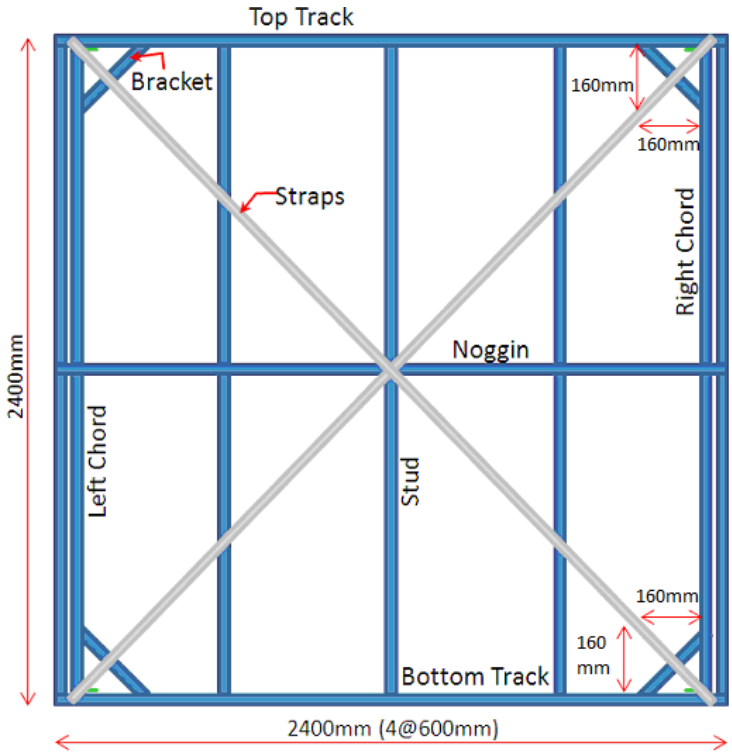


Figure 3. Strap-braced CFS frame.

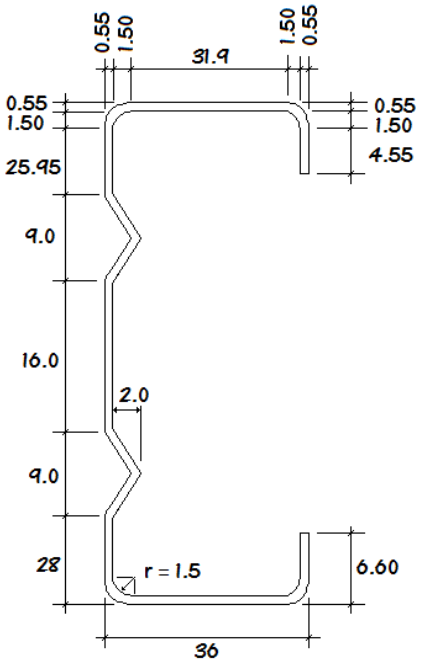


Figure 4. Detailed dimensions of stud C 90x36x0.55 in mm [34].

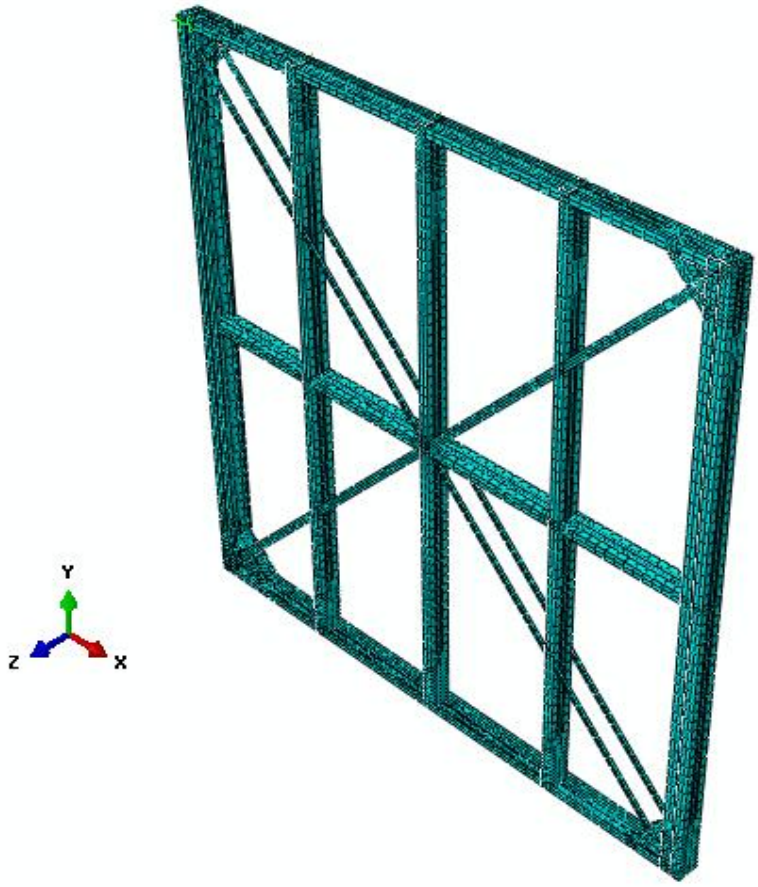


Figure 5. FE model of the CFS frame.

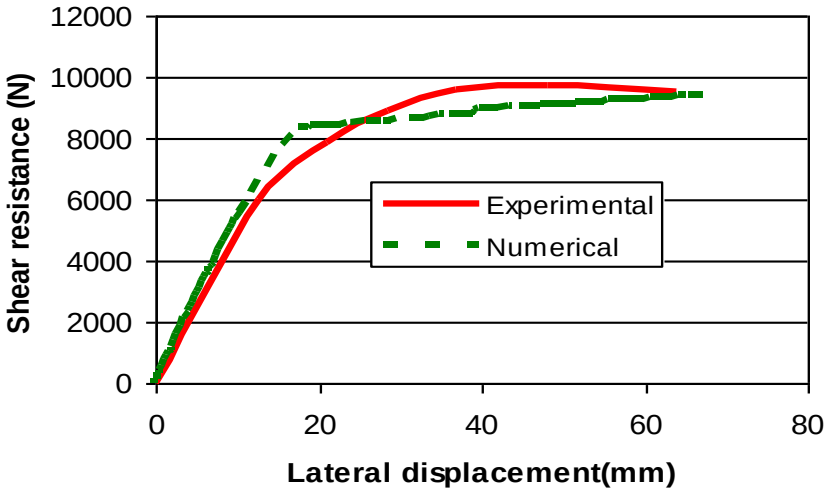


Figure 6: Pushover curves of the CFS frame.

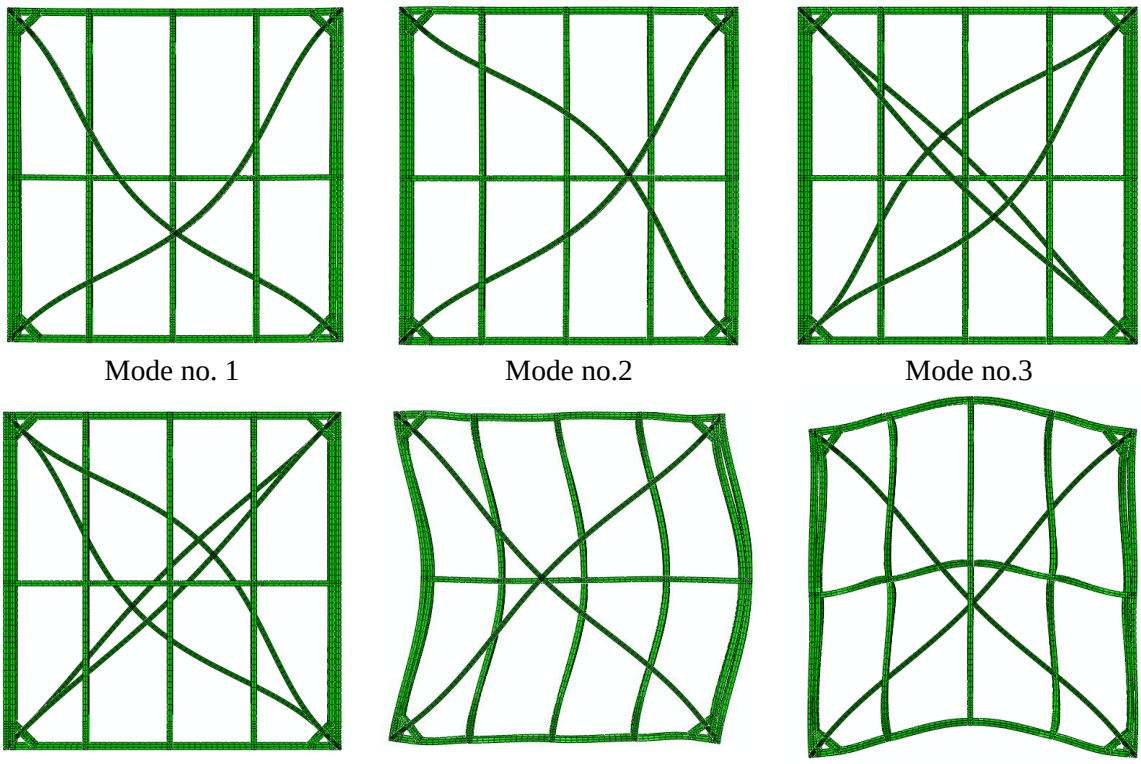


Figure 7. The first six mode shapes of the CFS frame.

*3.3 Optimization results*

The initial sensor candidate locations are shown in Figure 8 among them optimal sensor places would e selected for two, four and eight sensors. For this configuration, only the exterior chords and tracks have been chosen as the initial locations for sensor placement. In this case, 84 nodes were selected as the initial set of candidate sensor locations, giving 168 candidate DOFs due to lateral and vertical DOFs of each node. Based on the mode shape matrix calculated by finite element method (FEM), the above six IGA approaches which differ only in the chosen of objective function are implemented to select the best sensor locations among the initial candidate DOFs. The basic parameters of IGA are listed as Table 8:

Table 8: Basic parameters of IGA

| | | | |
|---|---|---|---|
| Number of target modes (n) | 2 | Parent size (Nkeep) | 20 |
| Number of sensors (m) | 2, 4, 8 | Offspring size (Npop-Nkeep) | 80 |
| Number of DOFs for sensor placement (s) | 168 | probability of mutation | 0.2 |
| Population size (Npop) | 100 | number of generations | 300 |

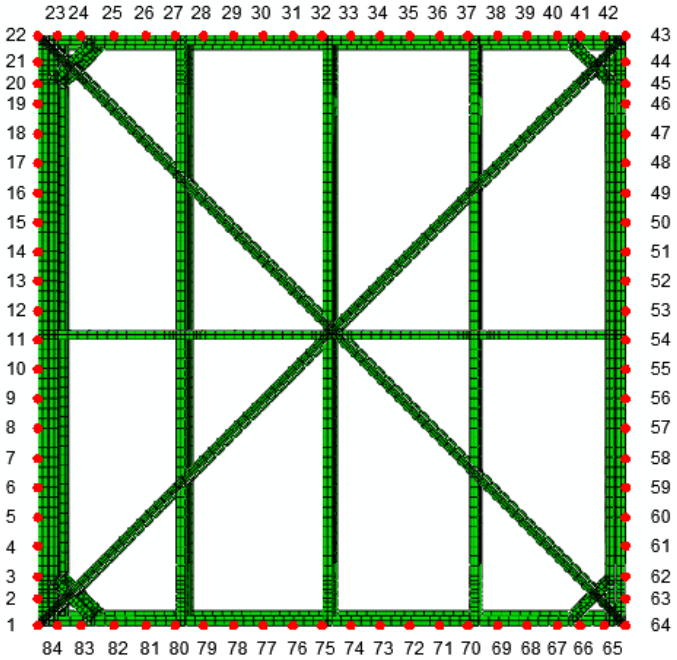


Figure 8: Initial candidates for sensor locations.

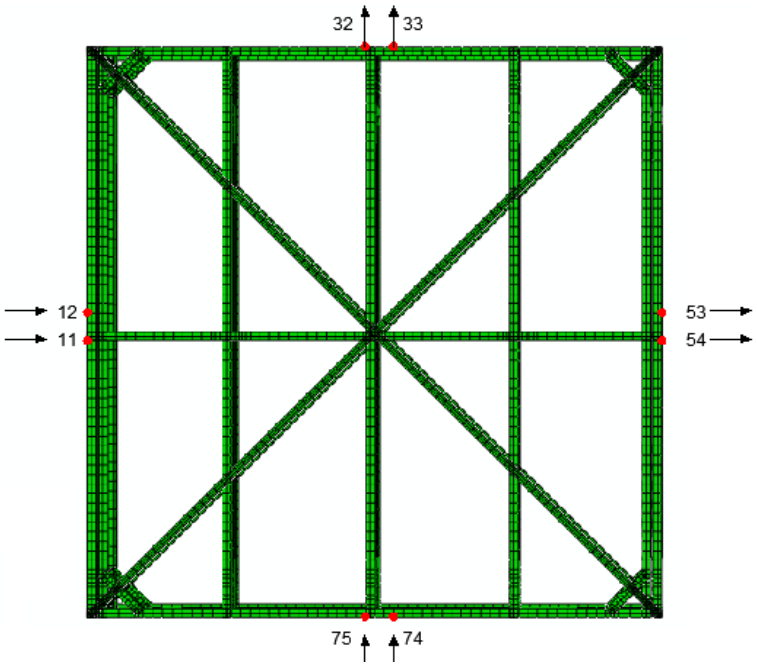


Figure 9: Sensor configuration by IGA with $fit_3$ for 8 sensors.

All the best results for two, four and eight sensor locations are listed and in Table 9. The best sensor placement for 8 sensors is also shown in Figure 9 based on the IGA with $fit_3$. In

order to evaluate the reliability of the above results, all the convergence curves of different fitness functions are shown as Figure 10 for maximum values and average values of the fitness functions. It is obvious that all the maximum fitness values tend to a constant quickly and along with increasing number of generations the average fitness values steadily tend to the maximum fitness values. It indicates a reasonable characteristic of convergence.

### *3.4 Comparison study*

To demonstrate the effectiveness of the IGA, the conventional methods of EFI, EFI-DPR and minMAC are performed and compared with the one proposed in this paper as follows:

#### *3.4.1 The EFI method*

In the EFI method, the procedure for OSP is to eliminate candidate sensor locations such that the determinant of the Fisher information matrix (FIM) is maximized. In order to achieve this, the effective independence (EFI) indices is proposed by Kammer [4] and evaluated by:

$$E_D = diag(\Phi\left[\Phi^T\Phi\right]^{-1}\Phi^T) = diag(QQ^T) \tag{15}$$

The bracketed term in the expression $P = \Phi\left[\Phi_m^T\Phi_m\right]^{-1}\Phi^T$ is a projection matrix made by the mode shape matrix $\Phi$, which can be decomposed by $\Phi = QR$, where Q is orthonormal matrix and $R$ is upper triangular matrix. EFI indices indicate the fractional contribution of each sensor placement to the independence of the target mode shapes. Therefore, to enhance the maximization of the determinant of FIM, an iterative algorithm is developed: at each step, the smallest term in $E_D$ is eliminated, and then corresponding row in $\Phi$ is also removed until the desired number of rows is obtained. One of the major limitations of EFI is that in order to have a non-singular FIM, the minimum sensor number employable must be equal to the target mode shape number $n$.

From this OSP technique, sensor networks have been determined for the studied frame as presented in Table 9.

#### *3.4.2 The EFI-DPR method*

As mentioned in section 2.2, by the EFI method, the sensor locations with low energy may be selected and therefore mode shape would be identified difficulty. The EFI-DPR method eliminates this problem by weighting the EFI indices with DPR defined by Eq. (8) [33]:

DPR calculates the average contribution of each candidate position to the mode shapes and changes of the $E_D$ vector expression as follows [33]:

$$E_D = diag(QQ^T)\Phi \otimes \Phi^T\Omega^{-1} \tag{16}$$

As shown in Table 9, this methodology gets a similar result to the EFI method for the

studied frame.

*3.4.3 The minMAC method*

Came and Dohrmann [6] presented the minMAC method for OSP based upon the modal assurance criterion (MAC). MAC is defined by Eq. (1) and provides a useful evaluation for the correlation of mode shapes. $MAC_{ij}$ represents the cosine of the angle between two vectors, hence the smaller the cosine, the more distinguishable the mode shape vectors. Therefore to achieve a set of sensors of well vector correspondence, the off-diagonal elements of MAC matrix must be minimized.

The results in Table 9 show that the sensor locations identified by the minMAC method are distributed asymmetrically in the entire frame.

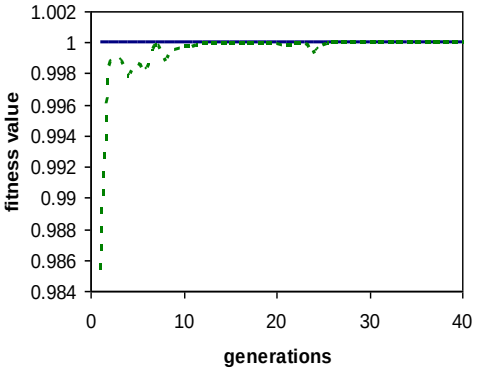


(a) m=8

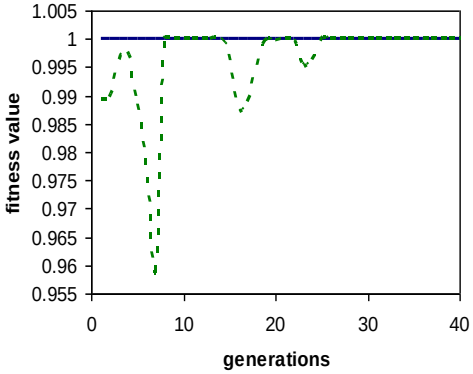


(b) m=8

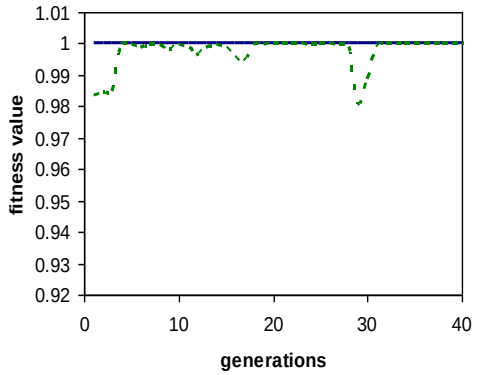


(a) m=4

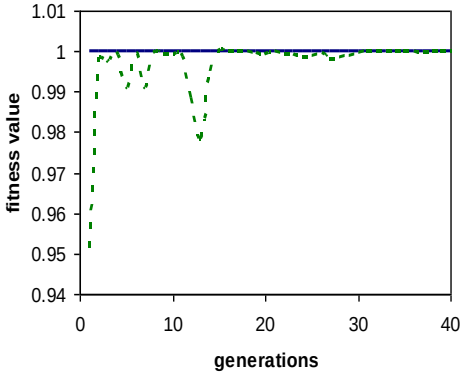


(b) m=4

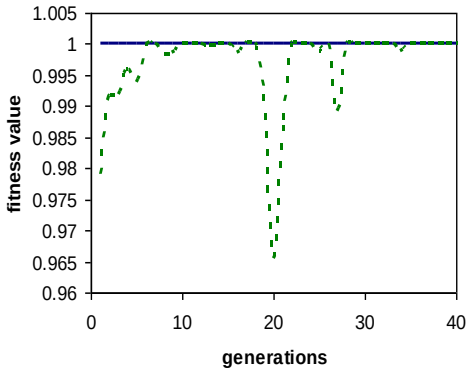


(a) m=2

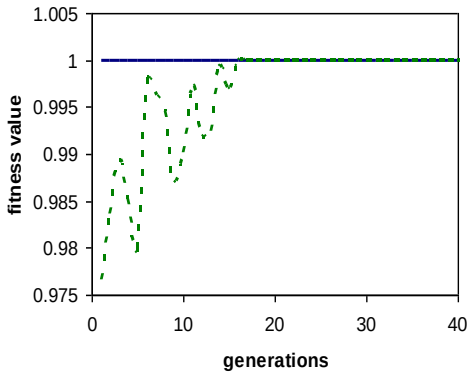


(b) m=2

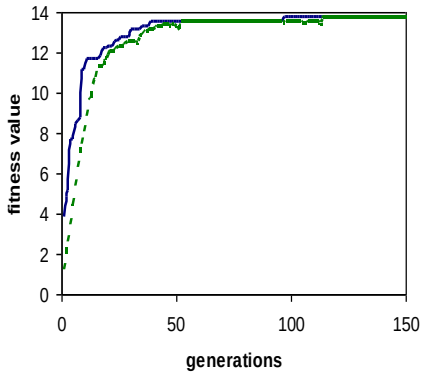


(c) m=8

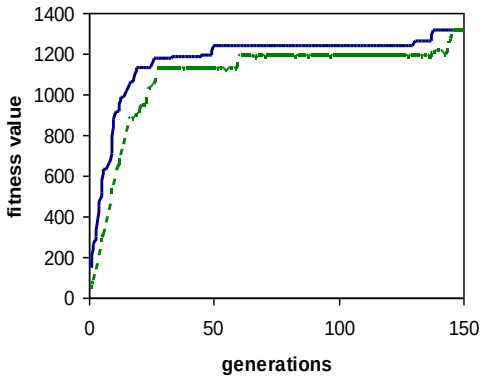


(d) m=8

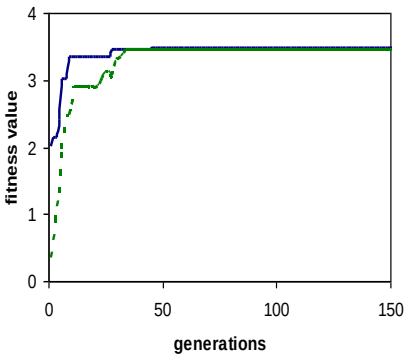


(c) m=4

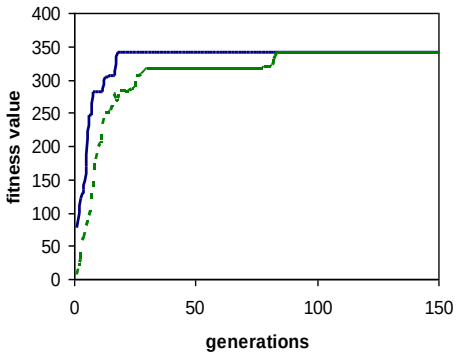


(d) m=4

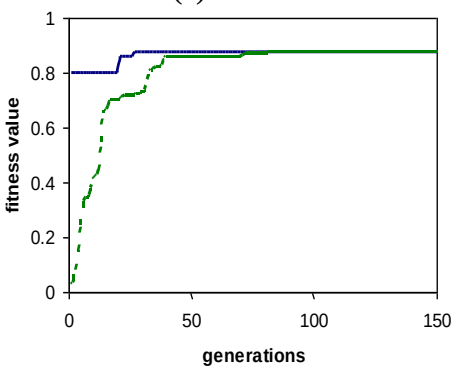


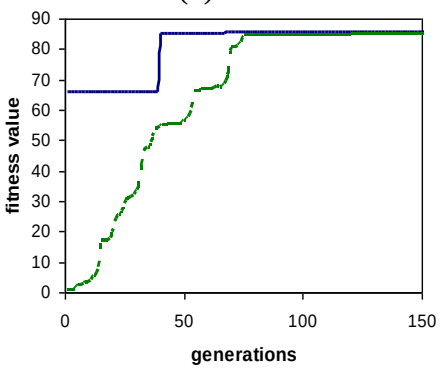

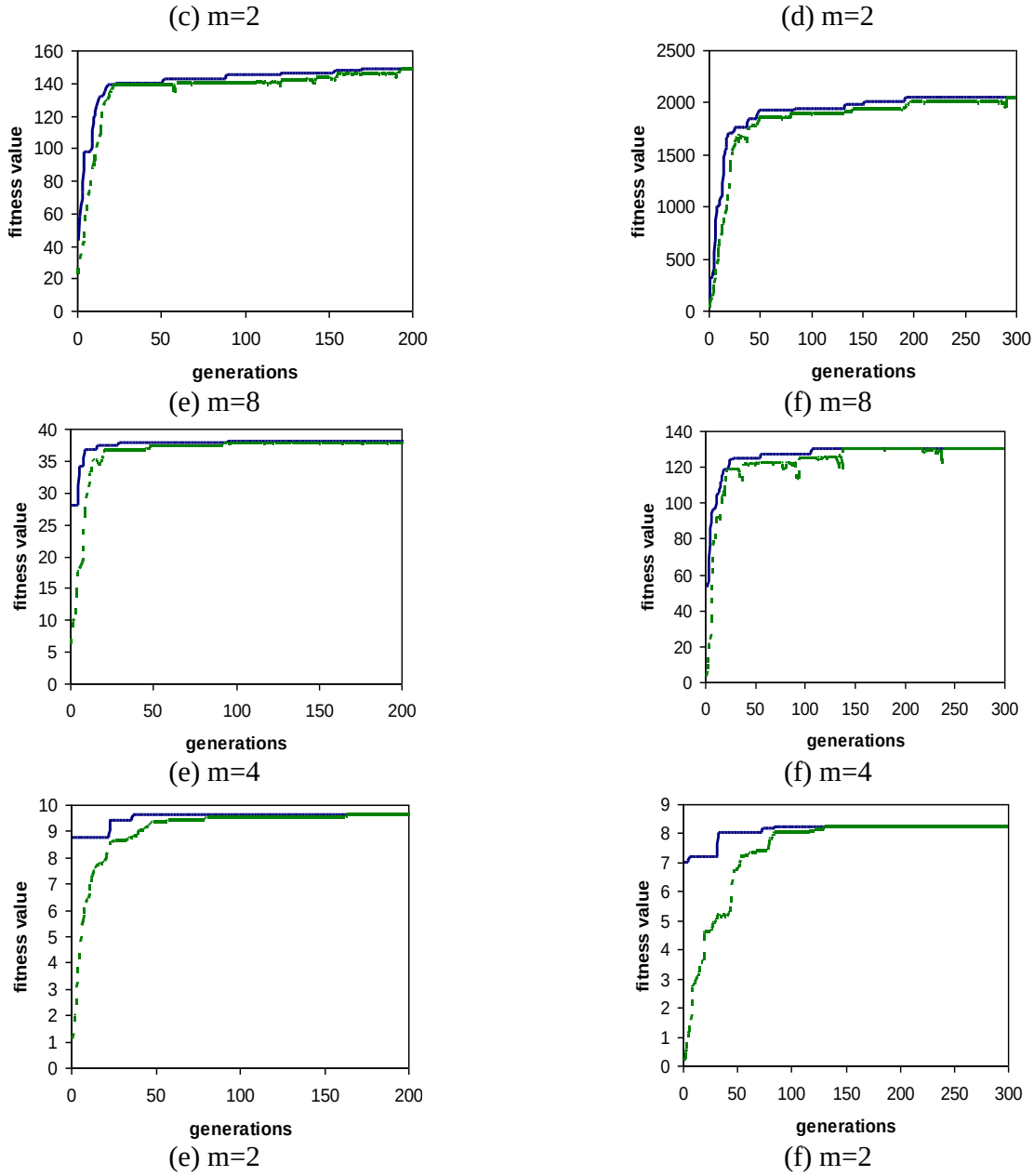


Figure 10. Convergence process of IGA with different fitness functions, a)$fit_1$,b)$fit_2$, c)$fit_3$, d)$fit_4$, e)$fit_5$, f)$fit_6$ for *m=8, 4, 2.*

## 4. CRITERIA- BASED EVALUATION OF THE OSP METHODS

In order to compare the capability of the aforementioned OSP techniques for identification of the vibration behaviour of the CFS frame, different criteria have been used: 1- Determinant, trace and SVD of FIM, 2- Maximum in off-diagonal terms (MOD) of MAC, 3-

Root mean square (RMS), and 4- SVD of mode shapes.

*4.1 Determinant, trace and SVD of FIM*

FIM is the inverse of the covariance matrix of estimators and indicates the volume of information acquired from mode shapes. In practice, different norms of the FIM are used as the criteria for the estimation of the amount of information. The determinant, the trace, and the minimum singular value of the FIM, are three common norms of FIM which are maximized to increase the information. That is to say, different sensor placement methods based on maximization of the trace, maximization of the determinant or maximization of the minimum singular value of the FIM will yield similar results for most cases [37].

The criteria of the FIM evaluating the sensor placement methods are listed in Table 10. All the methods, except the MAC-based methods, show good performance under these three criteria. As the number of sensors increased, the values of the norms of the FIM are increased too.

*4.2 Maximum in Off-Diagonal (MOD) terms of MAC*

The size of the off-diagonal elements of Modal Assurance Criterion (MAC) matrix could be another means to assess the capability of the chosen sensor locations to distinguish mode shapes accurately. The element values of the MAC matrix range between 0 and 1, where zero indicates that there is little or no correlation between the off-diagonal element $MAC_{ij}$ ($i \neq j$) and one denotes that there is a high degree of similarity between the modal vectors. The off-diagonal terms should be as small as possible for distinguishable mode shapes. Thus, the MOD of MAC provides a criterion for linear independency of mode shapes. In Table 10, the maximum off-diagonal term of MAC matrix is listed for comparison of the methods under consideration.

*4.3 Root Mean Square (RMS)*

RMS defined by Eq. (17) is a kind of criterion to assess the independency of mode shapes. But it is more general measurement than MOD of MAC.

$$RMS = \sqrt{\left(\sum_{i \neq j} \Phi_{ij}^2\right)}, \{i, j \in n | 1 \leq i \leq m, 1 \leq j \leq n\} \tag{17}$$

Similar to MOD, the smaller RMS indicates more independent of the mode shape vectors.

*4.4 Singular Value Decomposition (SVD)*

The SVD of the mode shape matrix specified at certain degrees of freedom provides another criterion of the capability of the sensor placement methods [38]. The criterion evaluates the ratio of the largest to the smallest singular value of the mode shape matrix as follows:

$$SVD = \frac{\sigma_1}{\sigma_m} \tag{18}$$

where $\sigma_1$ and $\sigma_m$ show the largest and smallest singular value of the mode shape matrix,

respectively. The lower limit of the SVD ratio is one and occurs in an ideal situation in which the mode shapes are orthonormal. The evaluation of the performance of the sensor placement methods using the SVD ratio criterion is shown in the Tables 10. Based on this criterion, almost all the methods show good performance for the number of 8 sensors. By decreasing the number of sensors, the value of SVD is rising in most cases.

Table 9: Optimal sensor placements for two, four and eight sensors.

| method | 2 | | 4 | | | | 8 | | | | | | | |
|---|---|---|---|---|---|---|---|---|---|---|---|---|---|---|
| $fit_1$ | 26 | 31 | 12 | 9 | 37 | 50 | 9 | 50 | 26 | 27 | 28 | 38 | 53 | 71 |
| | y | x | x | y | y | y | x | x | y | y | y | y | y | y |
| $fit_2$ | 50 | 77 | 53 | 56 | 71 | 74 | 13 | 14 | 37 | 57 | 5 | 17 | 38 | 68 |
| | x | y | x | x | y | y | x | x | x | x | y | y | y | y |
| $fit_3$ | 12 | 32 | 11 | 12 | 32 | 75 | 11 | 12 | 32 | 33 | 53 | 54 | 74 | 75 |
| | x | y | x | x | y | y | x | x | y | y | x | x | y | y |
| $fit_4$ | 12 | 32 | 11 | 12 | 32 | 75 | 11 | 12 | 32 | 33 | 53 | 54 | 74 | 75 |
| | x | y | x | x | y | y | x | x | y | y | x | x | y | y |
| $fit_5$ | 53 | 33 | 11 | 53 | 33 | 75 | 11 | 12 | 32 | 33 | 53 | 54 | 75 | 76 |
| | x | y | x | x | y | y | x | x | y | y | x | x | y | y |
| $fit_6$ | 53 | 75 | 11 | 53 | 32 | 75 | 11 | 12 | 32 | 33 | 53 | 54 | 75 | 76 |
| | x | y | x | x | y | y | x | x | y | y | x | x | y | y |
| EFI | 12 | 32 | 11 | 12 | 32 | 75 | 11 | 12 | 32 | 33 | 53 | 54 | 74 | 75 |
| | x | y | x | x | y | y | x | x | y | y | x | x | y | y |
| EFI-DPR | 12 | 32 | 11 | 12 | 32 | 75 | 11 | 12 | 32 | 33 | 53 | 54 | 74 | 75 |
| | x | y | x | x | y | y | x | x | y | y | x | x | y | y |
| MAC | 12 | 37 | 12 | 37 | 54 | 68 | 12 | 26 | 32 | 37 | 54 | 58 | 68 | 70 |
| | x | y | x | y | x | x | x | y | x | y | x | x | x | x |

Table 10: Results of sensor placement methods based on the criteria.

| method | Number of sensors | Determinant of FIM | Trace of FIM | SVD of FIM | MAC | RMS | SVD |
|---|---|---|---|---|---|---|---|
| $fit_1$ | 2 | 0.0022 | 0.1186 | 0.0225 | 0 | 0 | 2.0667 |
| | 4 | 0.2892 | 1.2568 | 0.3033 | 0 | 0.06460 | 1.7279 |
| | 8 | 1.7781 | 2.6703 | 1.2679 | 0 | 1.4303 | 1.0517 |
| $fit_2$ | 2 | 0.4297 | 1.3127 | 0.6242 | 0 | 0.0141 | 1.0502 |
| | 4 | 2.3318 | 3.0749 | 1.3587 | 0 | 1.1239 | 1.5166 |
| | 8 | 0.5809 | 2.5741 | 0.2499 | 0 | 1.5973 | 3.0494 |
| $fit_3$ | 2 | 0.8754 | 1.8719 | 0.9111 | 0.0005 | 0.0149 | 1.0269 |
| | 4 | 3.4775 | 3.7301 | 1.8355 | 0 | 1.6695 | 1.016 |
| | 8 | 13.7402 | 7.4148 | 3.6382 | 0 | 2.5444 | 1.0188 |
| $fit_4$ | 2 | 0.8754 | 1.8719 | 0.9111 | 0.0005 | 0.0149 | 1.0269 |
| | 4 | 3.4775 | 3.7301 | 1.8355 | 0 | 1.6695 | 1.016 |
| | 8 | 13.7402 | 7.415 | 3.6382 | 0 | 2.5444 | 1.0188 |

| | | | | | | | |
|---|---|---|---|---|---|---|---|
| $fit_5$ | 2 | 0.8484 | 1.8442 | 0.8792 | 0.0017 | 0.0283 | 1.0477 |
| | 4 | 3.4233 | 3.7023 | 1.7916 | 0.0007 | 1.6610 | 1.7916 |
| | 8 | 13.5178 | 7.3565 | 3.5701 | 0.0002 | 2.5329 | 1.0298 |
| $fit_6$ | 2 | 0.8609 | 1.8565 | 0.9010 | 0.0007 | 0.0206 | 1.0298 |
| | 4 | 3.4607 | 3.7211 | 1.8292 | 0.0001 | 1.6667 | 1.0170 |
| | 8 | 13.7402 | 7.415 | 3.6382 | 0 | 2.5444 | 1.0188 |
| EFI | 2 | 0.8754 | 1.8719 | 0.9111 | 0.0005 | 0.0149 | 1.0269 |
| | 4 | 3.4775 | 3.7301 | 1.8355 | 0 | 1.6695 | 1.016 |
| | 8 | 13.7402 | 7.4148 | 3.6382 | 0 | 2.5444 | 1.0188 |
| EFI-DPR | 2 | 0.8754 | 1.8719 | 0.9111 | 0.0005 | 0.0149 | 1.0269 |
| | 4 | 3.4775 | 3.7301 | 1.8355 | 0 | 1.6695 | 1.016 |
| | 8 | 13.7402 | 7.415 | 3.6382 | 0 | 2.5444 | 1.0188 |
| MAC | 2 | 9.2e-5 | 0.9504 | 9.8e-5 | 0 | 0.9748 | 98.6156 |
| | 4 | 0.0004 | 1.8915 | 0.0002 | 0 | 1.3753 | 85.5291 |
| | 8 | 0.7238 | 2.6930 | 0.3028 | 0 | 1.6342 | 2.8095 |

## 5. CONCLUSION

In this paper, an improved genetic algorithm (IGA) was adopted for the purpose of optimal sensor placement (OSP) for accurate modal identification of a strap-braced cold formed steel (CFS) frame. Based on different fitness functions, six approaches were considered to optimize the sensor locations. In addition to the proposed method, three conventional methods EFI, EFI-DPR and minMAC were applied for OSP of the frame. The results obtained from the proposed method and conventional methods are compared based on the criteria selected to access the effectiveness of the methods. The conclusions are summarized as follows:

- The IGA applied to the frame shows good convergence for all the fitness functions.
- Due to limited number of mode shapes for the studied frame, there are various configurations of sensor that can yield the maximum of the MAC-based fitness functions of $fit_1$ and $fit_2$. Therefore, the results of the IGA based on $fit_1$ and f$it_2$, as well as the result of minMAC method, are not recommended for final sensor network of the frame.
- The results of IGA for fitness functions of $fit_3$ and $fit_4$ which are based on EFI and EFI-DPR indices, respectively, are same as those obtained by conventional methods of EFI and EFI-DPR.
- The IGA methods by $fit_3$ and $fit_4$ as well as EFI and EFI-DPR are relatively useful and effective approaches based upon the evaluation criteria.
- The results of the methods based on fitness functions of $fit_5$ and $fit_6$ are similar to those based on $fit_3$ and $fit_4$, except for some limited DOFs.
- In comparison among fitness functions of $fit_3$ to $fit_6$, those based on EFI and EFI-DPR indices ($fit_3$ and $fit_4$) satisfy the criteria more than those based on ranking the mode shapes ($fit_5$ and $fit_6$). But all the mentioned methods yield reasonable results for optimal sensor locations of the frame.
- The overall deployment of the acceptable methods is satisfactory as the sensors locate

in a relatively regular fashion.

- The IGA proposed in this paper has the capability of solving OSP problem of the strap-braced CFS frame.

## REFERENCES


1. Papadimitriou C. Optimal sensor placement methodology for parametric identification of structural systems, Journal of Sound and Vibration, 2004; 278: 923-947.
2. Cherng AP. Optimal sensor placement for modal parameter identification using signal subspace correlation techniques, Mechanical Systems and Signal Processing, 2003; 17 (2): 361-378.
3. Kang F, Li JJ, Xu Q. Virus coevolution partheno-genetic algorithms for optimal sensor placement, Advanced Engineering Informatics, 2008; 22: 362–370.
4. Kammer DC. Sensor placement for on-orbit modal identification and correlation of large space structures, Journal of Guidance, Control and Dynamics, 1991; 14 (2): 251-259.
5. Lim KB. Method for optimal actuator and sensor placements for large flexible structures, Journal of Guidance, Control and Dynamics, 1992; 15(1): 49-57.
6. Came TG, Dohrmann CR. A modal test design strategy for model correlation, Proceedings of the 13th International Modal Analysis Conference, Nashville, Tennessee, USA, 1995, pp.927-933.
7. Kammer DC. Sensor set expansion for modal vibration testing, Mechanical Systems and Signal Processing, 2005; 19(4): 700-713.
8. Li DS, Li HN, Fritzen CP. The connection between effective independence and modal kinetic energy methods for sensor placement, Journal of Sound and Vibration, 2007; 305: 945-955.
9. Li DS, Fritzen CP, Li HN. Extended MinMAC algorithm and comparison of sensor placement Methods, Conference of 2008 IMAC-XXVI: International Modal Analysis Conference & Exposition on Structural Dynamics: Conference & Exposition on Structural Dynamics, Jacksonville, Florida, USA, 2008, on CD-ROM.
10. Li ZN, Tang J, Li QS. Optimal sensor locations for structural vibration measurements, Applied Acoustics, 2004; 65: 807-818.
11. Papadimitriou C. Pareto optimal sensor locations for structural identification, Computer Methods in Applied Mechanics and Engineering, Special Issue on Computational Methods in Stochastic Mechanics and Reliability Analysis, 2005; 194: 1655-1673.
12. Yao L, Sethares WA, Kammer DC. Sensor placement for on-orbit modal identification via a genetic algorithm, AIAA Journal, 1993; 31(10): 1922-1928.
13. Papadimitriou C, Beck JL, Au SK. Entropy- based optimal sensor location for structural model updating, Journal of Vibration and Control, 2000; 6(5): 781-800.
14. Vosoughifar HR, Shokouhi SKS. Health monitoring of LSF Structure via novel TTFD approach, Civil Structural Health Monitoring Workshop (CSHM-4), Berlin, Germany, 2012.

15. Vosoughifar HR, Shokouhi SKS, Farshadmanesh P. Optimal sensor placement of steel structure with UBF system for SHM using hybrid FEM-GA technique, Civil Structural Health Monitoring Workshop (CSHM-4), Berlin, Germany, 2012.
16. Abdullah MM, Richardson A, Jameel H. Placement of sensors/ actuators on civil structures using genetic algorithm, Earthquake Engineering and Structural Dynamics, 2001; 30(8): 1167-1184.
17. Huang WP, Liu J, Li HJ. Optimal sensor placement based on genetic algorithms, Engineering Mechanics, 2005; 22(1): 113-117.
18. Javadi AA, Farmani R, Tan TP, A hybrid intelligent genetic algorithm, Advanced Engineering Informatics, 2005; 19(4): 255-262.
19. Hwang SF, He RS. A hybrid real-parameter genetic algorithm for function optimization, Advanced Engineering Informatics, 2006; 20(1): 7-21.
20. Kubota N, Fukuda T, Shimojima K. Virus-evolutionary genetic algorithm for a self-organizing manufacturing system, Computers & Industrial Engineering Journal, 1996; 30(2): 1015-1026.
21. Kubota N, Shimojima K, Fukuda T. The role of virus infection in virus-evolutionary genetic algorithm, Proceedings of IEEE International Conference on Evolutionary Computation, Nagoya, Japan: IEEE, 1996, pp. 182-187.
22. Hu SC, Xu XF, Li XY. A Virus Coevolution genetic algorithm for project optimization scheduling, Journal of software, 2004; 15(1): 49-57.
23. Ning FH, Chen ZC, Xiong L. Decision model and algorithm of task coordination for collaborative logistics network, Control and Decision, 2007; 22(1): 109-112.
24. Yang Y, Gu ZQ, Hu L. The application of virus evolutionary genetic algorithm to dynamic path planning, Automotive Engineering, 2007; 29(1): 67–70.
25. Liu W, Gao WC, Sun Y, Xu MJ. Optimal sensor placement for spatial lattice structure based on genetic algorithms, Journal of Sound and Vibration, 2008; 317: 175-189.
26. Yi TH, Li HN, Gu M. Optimal sensor placement for health monitoring of high-rise structure based on genetic algorithm, Mathematical Problems in Engineering, 2011; Article ID 395101, 12 pages, doi: 10.1155/2011/395101.
27. Y TH, Li HN, Gu M. Optimal sensor placement for structural health monitoring based on multiple optimization strategies, The Structural Design of Tall and Special Buildings, 2011; 20: 881–900.
28. Haupt RL, Haupt SE. *Practical Genetic Algorithms*, John Wiley & Sons, 2nd Edition, 2004, 253 pp.
29. Holland JH. *Adaptation in Natural and Artificial Systems*, Ann Arbor: University of Michigan Press, 1975.
30. Goldberg DE. *Genetic Algorithms in Search, Optimization, and Machine Learning*, Addison-Wesley Longman Publishing Co., Inc. Boston, MA, USA, 1989.
31. Guo HY, Zhang L, Zhang LL, Zhou JX. Optimal placement of sensors for structural health monitoring using improved genetic algorithms, Smart Materials and Structures, 2004; 13: 528-534.
32. Clough RW, Penzien J. *Dynamics of Structures*, McGraw Hill, 2nd edition, New York, 1993.
33. Worden K, Burrows AP. Optimal sensor placement for fault detection, Engineering

Structures, 2001; 23: 885-901.
34. Zeynalian M, Ronagh HR, Experimental study on seismic performance of strap-braced cold-formed steel shear walls, Advances in Structural Engineering, 2013; 16.
35. Abaqus 6.11. Abaqus/ CAE user's manual. 2011.
36. Zeynalian M, Ronagh HR. A numerical study on seismic performance of strap-braced cold formed steel shear walls, Thin- walled structures, 2012; 60: 229–238.
37. Basseville M, Benveniste A, Moustakides GV, Rougee A. Optimal sensor location for detecting changes in dynamic behavior, Ieee Transactions on Automatic Control, 1987; 32: 1067-1075.
38. Golub GH, Van Loan CF. *Matrix Computations*, Johns Hopkins University Press, 1996.